

# Sudden chaotic transitions in an optically injected semiconductor laser

Sebastian Wieczorek

Department of Physics and Astronomy, Vrije Universiteit Amsterdam, De Boelelaan 1081, 1081 HV Amsterdam, The Netherlands

Bernd Krauskopf

Department of Engineering Mathematics, University of Bristol, Bristol BS8 1TR, UK

Daan Lenstra

Department of Physics and Astronomy, Vrije Universiteit Amsterdam, De Boelelaan 1081, 1081 HV Amsterdam, The Netherlands

Received February 15, 2001

We study sudden changes in the chaotic output of an optically injected semiconductor laser. For what is believed to be the first time in this system, we identify bifurcations that cause abrupt changes between different chaotic outputs, or even sudden jumps between chaotic and periodic output. These sudden chaotic transitions involve attractors that exist for large regions in parameter space. © 2001 Optical Society of America

OCIS codes: 140.5960, 190.3100.

Chaotic behavior of semiconductor laser systems was viewed as something amazing from a fundamental point of view but also as a nuisance to be engineered away in applications. However, since semiconductor lasers were proposed for chaotic communication schemes,<sup>1</sup> their chaotic properties have turned out to be potentially useful and now demand more attention.

A semiconductor laser subject to optical injection is known to produce a large variety of dynamic behaviors, including complex and chaotic dynamics,<sup>2-7</sup> and the use of a semiconductor laser for chaotic communication schemes has been suggested<sup>8</sup> and studied.<sup>9</sup> This laser system is well described by the three-dimensional rate equations<sup>7</sup>

$$\begin{aligned} \dot{E} &= K + \left[ \frac{1}{2} (1 + i\alpha)n - i\omega \right] E, \\ \dot{n} &= -2\Gamma - (1 + 2Bn)(|E|^2 - 1), \end{aligned} \quad (1)$$

which describe the complex electric field,  $E = E_x + iE_y$ , and the population inversion,  $n$ , of an injected semiconductor laser. The two most important parameters are the injected field strength,  $K$ , and the detuning,  $\omega$ , from the solitary laser frequency, which both can be easily adjusted in an experiment. The linewidth-enhancement factor,  $\alpha$ , was fixed at  $\alpha = 2$  in this Letter, and the other scaled parameters,  $B$  and  $\Gamma$ , were set to the realistic values  $B = 0.015$  and  $\Gamma = 0.035$ . All scaled quantities can be related to experimental laser parameters.<sup>7</sup>

All results presented here were obtained by use of Eqs. (1), which define a dynamical system with the three-dimensional  $(E, n)$  space as its phase space. There are other techniques for studying complex behavior in dynamical systems,<sup>5,10</sup> but Eqs. (1) are particularly suited for the use of advanced tools from bifurcation theory.<sup>7,11</sup> This approach allows us to find sudden chaotic transitions and determine how they are embedded in a wider picture of bifurcations.<sup>7</sup> Specifically, we detect and follow<sup>12</sup> in the

$(K, \omega)$  parameter plane changes (bifurcations) in the laser's dynamics. Furthermore, we compute representative phase portraits<sup>13</sup> and stable and unstable manifolds.<sup>14</sup>

Figure 1 presents bifurcation curves in the  $(K, \omega)$  plane that divide this parameter space into regions of different dynamics. Supercritical bifurcations of attractors are shown as black curves, and subcritical bifurcations of unstable objects are shown as gray curves. The superscripts denote multiples of the base period of bifurcating periodic orbits.

An attracting equilibrium is born along the black part of the saddle-node bifurcation curve, SN. This equilibrium corresponds to stable laser output at the injected light frequency and exists inside the locking range bounded by SN and H in Fig. 1. When H is crossed, the relaxation oscillation becomes undamped in a Hopf bifurcation. New periodic orbits can be created in the saddle node of limit-cycle bifurcation SL. These oscillations may bifurcate further, for example, undergoing successive period doublings along

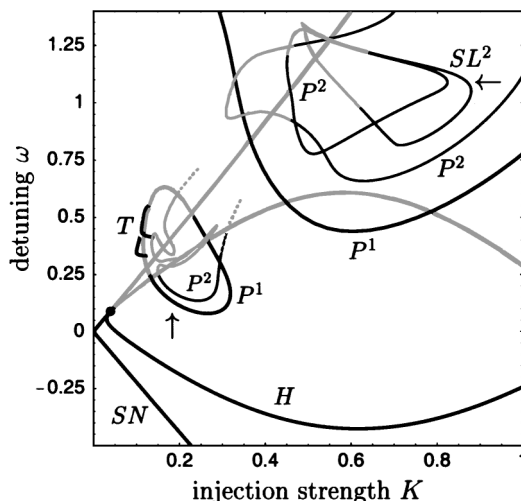


Fig. 1. Bifurcation diagram in the  $(K, \omega)$  plane.

curves  $P^1$  and  $P^2$ , or giving rise to quasi-periodic oscillations in torus bifurcations T.

This Letter is concerned with sudden chaotic transitions inside regions of chaos. We concentrate on the parameter regions inside the two period-doubling bubbles in Fig. 1. These chaotic regions are not homogeneously filled with one type of chaos as was experimentally shown for a CO<sub>2</sub> laser with internal modulation.<sup>4</sup> Instead, there is a complicated structure with different types of chaotic laser output and periodic windows. We show that, as the parameters are changed, chaotic output may abruptly change from one type to another or even suddenly disappear. The changes in chaotic dynamics that we discuss here are robust phenomena caused by unnested islands of period doublings, as will be reported in future work.

To illustrate these transitions, we present all relevant information for each fixed value of the parameters: the attractor as a projection onto the complex  $E$  plane, the corresponding attractor in the Poincaré section  $\{n = 0\}$ , the time series of the intensity,  $I = |E|^2$ , and the optical spectrum. (Time is measured in units of the relaxation-oscillation frequency of the free-running laser.) This representation facilitates comparisons with experimental data that, for semiconductor lasers, are available only in the form of spectra because of the fast time scales involved. The data were obtained by numerical integration of Eqs. (1).

To find the parameters for which chaotic transitions occur, we use Fig. 1 as our guide. There exists a region of chaotic laser output for parameters inside the small period-doubling bubble bounded by curve  $P^1$  (middle left of Fig. 1). When one crosses curve T, quasi-periodic oscillations are excited that then break up into chaos. However, the same chaotic region can be entered from below in a period-doubling route to chaos. Note that a chaotic attractor created directly after period doublings is usually small compared with a chaotic attractor that results from the breakup of a torus.<sup>15</sup> Therefore, there must be a bifurcation mechanism that causes the change from one type of chaos to the other.

This mechanism is illustrated in Fig. 2, in which the chaotic attractor suddenly increases its size dramatically in an interior crisis.<sup>16</sup> The chaotic attractor [Fig. 2(a2)] (created after a sequence of period doublings) has a fractal dimension slightly greater than 1. This attractor has a mixed spectrum, consisting of a broad contribution together with strong periodic peaks [Fig. 2(a3)]. Increasing  $K$  by just a bit results in a sudden change of the chaotic attractor, with a jump to a much larger fractal dimension [Fig. 2(b2)]. The spectrum is not mixed any longer, and the broad contribution now dominates [Fig. 2(b3)].

To determine the mechanism that creates the sudden change in the chaotic dynamics in Fig. 2, we plot in Fig. 3 the stable (gray curves) and unstable (black curves) manifolds<sup>14</sup> of a saddle orbit of period three (filled circles). In each part of the figure the unstable manifold accumulates on a chaotic attractor. Initially [Fig. 3(a)] the stable and unstable manifolds do not intersect, but then the stable manifold hits the chaotic attractor by forming a homoclinic tangency with the

unstable manifold [Fig. 3(b)]. Finally, the manifolds cross and form a homoclinic tangle [Fig. 3(c)]. This results in a dramatic change in the size of the chaotic attractor. The organization of the manifolds in Fig. 3 clearly shows that we found an interior crisis.<sup>16</sup>

The investigation of the bifurcation structure inside the bigger region bounded by curve  $P^1$  (top right corner of Fig. 1) reveals the existence of a bifurcation curve,  $SL^2$ , that creates a period-two oscillation within the chaotic region. In Fig. 4 we fix  $\omega = 1.1$ , start with the period-two orbit, and decrease the injection strength,  $K$ . This choice of parameters reveals a different transition called a boundary crisis.<sup>16</sup> Before the bifurcation there is bistability: A chaotic attractor (gray) coexists with a periodic orbit (black) [Figs. 4(a1) and 4(a2)]. In other words, the laser is able to produce either chaotic or periodic output for the same parameter settings, depending on the initial condition. Notice that the time series and the spectrum in Figs. 4(a3)

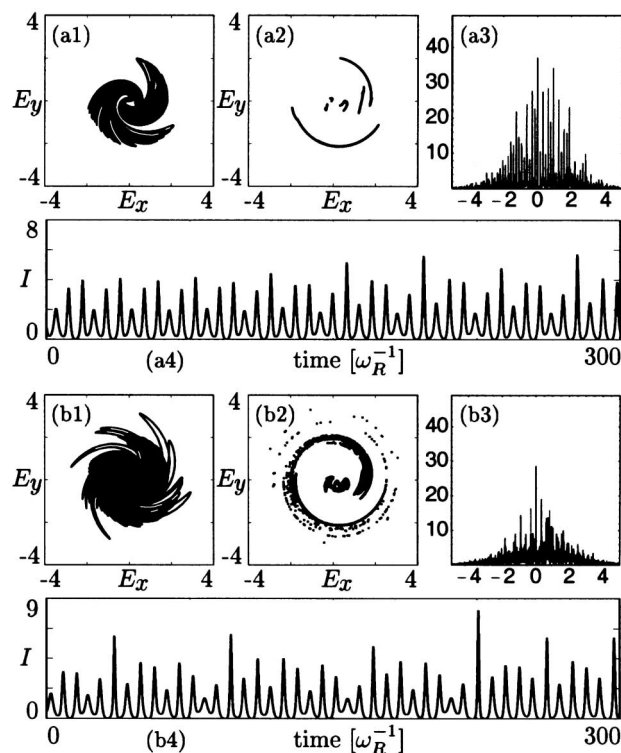


Fig. 2. Sudden growth of the chaotic attractor owing to an interior crisis when  $\omega =$  increases from (a1)–(a4) 0.257 to (b1)–(b4) 0.2595 for  $K = 0.19$  (indicated in Fig. 1 by a vertical arrow).

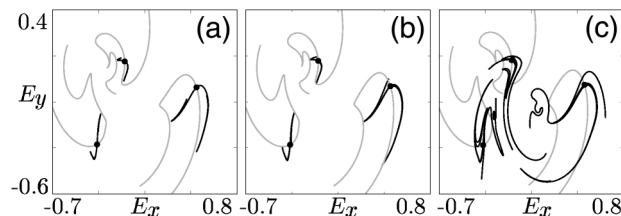


Fig. 3. Organization of the stable (gray) and unstable (black) manifolds in the Poincaré section  $\{n = 0\}$ : (a) before, (b) at, and (c) after an interior crisis. Here  $K = 0.19$  is fixed (indicated in Fig. 1 by a vertical arrow), and (a)  $\omega = 0.255$ , (b)  $\omega = 0.257$ , (c)  $\omega = 0.2595$ .

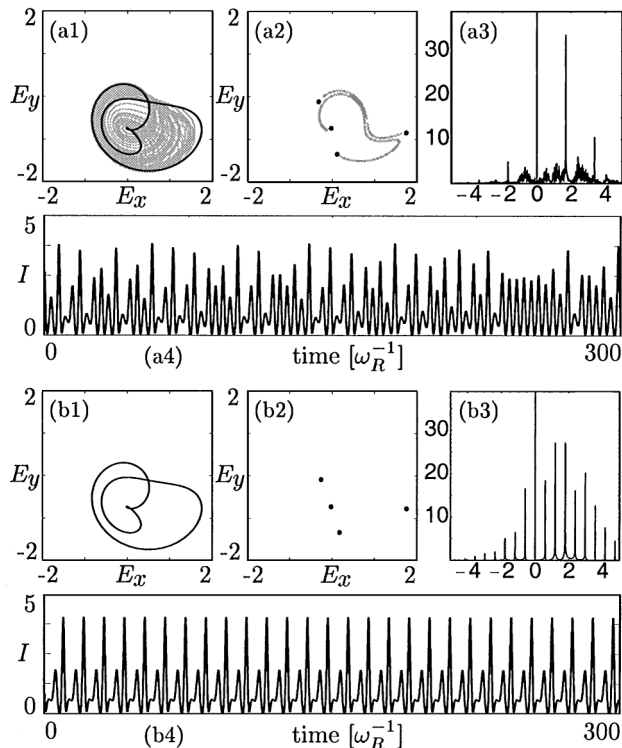


Fig. 4. Sudden destruction of a chaotic attractor owing to a boundary crisis when  $K$  decreases from (a1)–(a4) 0.84 to (b1)–(b4) 0.835 for fixed  $\omega = 1.1$  (indicated in Fig. 1 by a horizontal arrow).

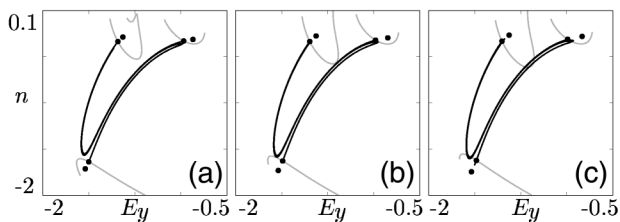


Fig. 5. Organization of the stable (gray) and unstable (black) manifolds in the Poincaré section  $\{E_x = 0\}$ : (a) before, (b) at, and (c) after a boundary crisis. Here  $\omega = 1.1$  is fixed (indicated in Fig. 1 by a horizontal arrow) and (a)  $K = 0.85$ , (b)  $K = 0.839$ , (c)  $K = 0.83$ .

and 4(a4), respectively, are for the chaotic attractor only. The chaotic attractor is destroyed when it hits the boundary between the two basins of attraction of the coexisting attractors. After this, the periodic orbit is the only attractor, and the laser produces periodic output [Figs. 4(b1)–4(b3)].

To determine the mechanism that creates this sudden transition, we plot in Fig. 5 the stable (gray) and unstable (black) manifolds of the saddle orbit of period two (filled circles). Initially the stable manifold of this orbit forms the boundary between the basins of attraction of the periodic orbit and the chaotic attractor [Fig. 5(a)]. The chaotic attractor then hits the boundary [Fig. 5(b)] by forming a homoclinic tangency with the unstable manifold. The chaotic attractor is destroyed in the process, and the periodic orbit remains

as the only attractor [Fig. 5(c)]. This organization of manifolds clearly shows that we found a boundary crisis.<sup>16</sup>

In conclusion, on the basis of our bifurcation analysis one should expect chaotic transitions, which are different from familiar transitions within a period-doubling cascade,<sup>4</sup> in an injected diode laser. Moreover, we have used modern tools from bifurcation theory that will facilitate experimental exploration of these transitions.

Studying transitions of chaotic attractors in optically injected semiconductor lasers is of strategic interest for applications using chaotic signals. We briefly mention two points concerning the sudden transitions discussed here. First, one can obtain switching between two different chaotic signals (chaos shift keying) for reliable and safe transmission of information by changing parameter values near an interior crisis. Second, using chaotic signals close to a boundary crisis may be dangerous, in that a small parameter variation may lead to loss of the chaotic attractor and to periodic laser output instead.

The research of S. Wieczorek was supported by the Foundation for Fundamental Research on Matter, which is financially supported by the Netherlands Organization for Scientific Research. B. Krauskopf's e-mail address is b.krauskopf@bristol.ac.uk.

## References

1. C. R. Mirasso, P. Colet, and P. Garcia-Fernández, *IEEE Photon. Technol. Lett.* **8**, 299 (1996).
2. F. T. Arecchi, R. Meucci, G. Puccioni, and J. Tredicce, *Phys. Rev. Lett.* **49**, 1217 (1982).
3. J. R. Tredicce, F. T. Arecchi, G. L. Lippi, and G. P. Puccioni, *J. Opt. Soc. Am. B* **2**, 173 (1985).
4. D. Dangoisse, P. Glorieux, and D. Hennequin, *Phys. Rev. Lett.* **57**, 2657 (1986).
5. H. G. Solari, E. Eschenazi, R. Gilmore, and J. Tredicce, *Opt. Commun.* **46**, 64 (1983).
6. T. Erneux, V. Kovanis, A. Gavrielides, and P. M. Alsing, *Phys. Rev. A* **53**, 4372 (1996).
7. S. Wieczorek, B. Krauskopf, and D. Lenstra, *Opt. Commun.* **172**, 279 (1999).
8. V. Annovazzi-Lodi, S. Donati, and M. Manna, *IEEE J. Quantum Electron.* **30**, 1537 (1994).
9. H. F. Chen and J. M. Liu, *IEEE J. Quantum Electron.* **36**, 27 (2000).
10. G. B. Mindlin, X. J. Hou, H. G. Solari, R. Gilmore, and N. B. Tufillaro, *Phys. Rev. Lett.* **64**, 2350 (1990).
11. B. Krauskopf and D. Lenstra, *AIP Conf. Proc.* **548**, 1 (2000).
12. E. Doedel, T. Fairgrieve, B. Sandstede, A. Champneys, Yu. Kuznetsov, and X. Wang, "AUTO 97," <http://indy.cs.concordia.ca/auto/main.html>.
13. A. Back, J. Guckenheimer, M. R. Myers, F. J. Wicklin, and P. A. Worfolk, *Not. Am. Math. Soc.* **39**, 303 (1992).
14. B. Krauskopf and H. M. Osinga, *J. Comp. Phys.* **146**, 404 (1998).
15. B. Krauskopf, S. Wieczorek, and D. Lenstra, *Appl. Phys. Lett.* **77**, 1611 (2000).
16. C. Grebogi, E. Ott, and J. A. Yorke, *Phys. Rev. Lett.* **48**, 1507 (1982).